Fluid Dynamics Research

PAPER

The Darrieus–Landau instability of premixed flames

To cite this article: Moshe Matalon 2018 *Fluid Dyn. Res.* **50** 051412

IOP Publishing | The Japan Society of Fluid Mechanics Fluid *Dynamics* Research

Fluid Dyn. Res. **50** (2018) 051412 (23pp) https://doi.org/10.1088/1873-7005/aab510

The Darrieus–Landau instability of premixed flames

Moshe Matalon

Department of Mechanical Science and Engineering University of Illinois at Urbana-Champaign, Urbana, IL 61801, United States of America

E-mail: matalon@illinois.edu

Received 3 January 2018
Accepted for publication 8 March 2018
Published 10 August 2018

Communicated by Pinhas Bar-Yoseph

Abstract

The most prominent intrinsic flame instability is the hydrodynamic, or Darrieus–Landau (DL) instability, that results from the gas expansion caused by the heat released during combustion, which induces hydrodynamic disturbances that enhance perturbations of the flame front. The DL instability has many ramifications in premixed combustion; it promotes the creation of corrugated flames with relatively sharp edges pointing towards the burned gas. In this presentation, we first review the developments that led to a better understanding of the roles of viscosity, heat conduction and species diffusion on the flame stability. This includes the work of Markstein that attempted to phenomenologically improve the Darrieus and Landau analyses, and the asymptotic studies that provided an explicit dependence on the physical parameters. We then discuss the nonlinear flame development starting with the weakly-nonlinear analytical studies and proceeding with the more recent fully-nonlinear numerical results. We show that, unlike the implication that may be inferred from the original publications of Darrieus and Landau that premixed flames as a result of the instability will always appear as turbulent flames, the instability leads to the formation of cusp-like conformations with elongated intrusions pointing toward the burned gas region. These structures are *stable* and, because of their larger surface area, propagate at a speed that is substantially faster than the laminar flame speed. Finally, we show that the DL instability remains relevant in turbulent flames, but their influence appears limited to weak-to-moderate turbulence intensity flows.

Keywords: hydrodynamic theory of premixed flames, Darrieus–Landau instability, hydrodynamic instability, thermo-diffusive instabilities, flame speed and flame stretch

(Some figures may appear in colour only in the online journal)

1. Introduction

The hydrodynamic instability, discovered independently by Darrieus (1938) and Landau (1944) nearly eighty years ago is the most consequential instability in premixed combustion. Known also as the Darrieus–Landau (DL) instability, it is a consequence of the amplification of the flame front by hydrodynamic disturbances induced by the gas expansion that results from the heat released during combustion. Although the linear stability analyses of Darrieus and Landau raise a number of fundamental questions, primarily their conjectures that the flame speed along the flame surface is constant and independent of the influences of the diffusion processes occurring inside the flame zone, the instability is nevertheless present and dominant in large scale flames. It is responsible for the formation of sharp creases and crests pointing towards the burned gas region, for the convex curving of flames propagating in narrow tubes, and for the self-wrinkling of the surface of large expanding flames.

The simplest problem of premixed combustion is arguably the propagation of a planar flame into a quiescent mixture. The flame propagates at a constant speed determined uniquely by the thermo-mechanical properties of the combustible mixture. In a frame of reference attached to the flame the problem is steady, but due to the highly nonlinear reaction term appearing in the governing equations an exact solution describing the flame structure and determining the flame speed is not available. Insight into the nature of the flame structure has emerged since the work of Mallard and Chatelier (1883), but were firmly established only in recent years by treating the overall activation energy large in comparison with the enthalpy of the mixture. An analytical solution in this asymptotic limit was first presented heuristically by Zel'dovich and Frank-Kamenetsky (1938) and later formally using matched asymptotic expansions by Bush and Fendell (1970). Although the availability of such a solution appears useful for stability considerations, the perturbed eigenvalue problem, due to the variation of the flow properties with distance through the flame, comprises of a coupled system of *variable coefficient* equations, which is a formidable task even when treated numerically. The search for an explicit dispersion relation that exhibits a dependence on the various controlling parameters affecting the flame propagation necessitates the construction of *simplified models* that possess tractable solutions that can then be tested for stability.

In this presentation, we review the main developments that led to the current understanding of the nature of the hydrodynamic instability, starting from the work of Darrieus and Landau who considered the flame as a structureless surface separating burned and unburned gases and moving at a constant speed relative to the flow, the subsequent work of Markstein (1964) who introduced phenomenologically a correction to the flame speed that accounts for effects arising from the internal flame region, and the more rigorous asymptotic studies by Pelce and Clavin (1982), Frankel and Sivashinsky (1982) and Matalon and Matkowsky (1982) that systematically accounted for the internal structure of the flame using a multi-scale approach. All three asymptotic studies led to a correction term to the DL dispersion relation which, except for notation and non-dimensionalization, is identical[1]. They differ only by their mathematical approach; Pelce and Clavin and Frankel and Sivashinsky linearized the governing equations about the planar flame solution, then used a multi-scale approach to incorporate the effects of diffusion to the hydrodynamic problem. Matalon and Matkowsky, on the other hand, derived first a *general model* for treating the flame as a thin interior layer separating the fresh combustible mixture from the burned gases, and then used their model to examine the stability of planar flames.

[1] The work of Pelce and Clavin also incorporated the effect of gravity which, as pointed out by Landau acts to stabilize the long wavelength disturbances; gravity will not be discussed in this paper.

The result of all three studies explicitly exhibit the influence of diffusion on the flame propagation, showing that it often acts to stabilize the short wavelength disturbances.

The general model derived by Matalon and Matkowsky (1982) and referred below as the *hydrodynamic model* has been cast in a coordinate-free form (Matalon and Matkowsky 1983) and generalized to account for temperature-dependent transport, differential and preferential diffusion (i.e., non-unity and distinct Lewis numbers), and effects due to stoichiometry and reaction orders (Matalon *et al* 2003). The mathematical formulation consists of a nonlinear free-boundary problem; the flame is represented by a surface separating burned from unburned gases, with different densities and temperatures, and propagates relative to the fresh mixture at a speed that depends on the local stretch rate modulated by a Markstein length that mimics the influences of diffusion and chemical reaction occurring inside the flame zone. The flame propagation is therefore affected by the local flow conditions through the flame stretch, which consists of the curvature of the flame surface and the underlying hydrodynamic strain it experiences, and by the local mixture composition through the Markstein length. The flow field is modified in turn by the gas expansion resulting from the increase in temperature caused by the heat released. The hydrodynamic model remains valid when the flow is either laminar or turbulent, and has been therefore used to investigate the nonlinear consequences of the DL instability in a laminar setting (Rastigejev and Matalon 2006, Creta and Matalon 2011) and its effect on turbulent flames (Creta and Matalon 2011, Fogla *et al* 2015, 2017).

2. The Darrieus and Landau analyses

Darrieus (1938) and Landau (1944) were the first to address the stability of planar flames. The flame in their description is a structureless interface separating fresh combustible gas mixture from burned gas products. The flow field on either side of the flame front is described by the Euler equations of an inviscid, incompressible gas, and must satisfy the Rankine–Hugoniot (RH) jump relationships corresponding to statements of mass and momentum and energy conservations across the flame. The mathematical formulation is completed by specifying the *flame speed* defined as the propagation speed relative to the flow, which Darrieus and Landau assumed to be constant along the flame surface.

Let the flame front be described mathematically by a function $F(\mathbf{x}, t) = 0$, with $F < 0$ identifying the unburned gas region and $F > 0$ the burned gas region, the flame speed S_f is defined from $S_f \equiv -V_f + v_n^*$, where v_n^* is the normal component of the gas velocity just ahead of the flame (the *, here and thereafter denotes conditions at the flame front on the unburned side), and

$$\mathbf{n} = \frac{\nabla F}{|\nabla F|}, \qquad V_f = -\frac{1}{|\nabla F|}\frac{\partial F}{\partial t}$$

are, respectively, the unit normal to the flame surface pointing towards the burned gas and the normal propagation speed (in the laboratory frame) of the interface; see figure 1. The Euler equations are given by

$$\nabla \cdot \mathbf{v} = 0, \qquad \rho\left(\frac{\partial \mathbf{v}}{\partial t} + (\mathbf{v}\cdot\nabla)\mathbf{v}\right) = -\nabla p \tag{1}$$

where $\mathbf{v}$ is the velocity vector, p is the pressure, and ρ the density represented by ρ_u and ρ_b in the unburned/burned regions, respectively. The RH jump relations are given by

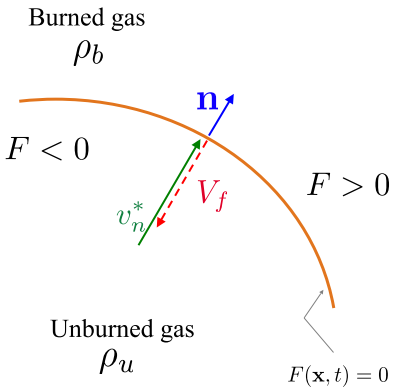

Figure 1. Schematic of the flame front and its geometrical properties.

$$\begin{aligned} [\![\rho(\mathbf{v}\cdot\mathbf{n} - V_f)]\!] &= 0 \\ [\![\mathbf{n}\times(\mathbf{v}\times\mathbf{n})]\!] &= 0 \\ [\![p + \rho(\mathbf{v}\cdot\mathbf{n})(\mathbf{v}\cdot\mathbf{n} - V_f)]\!] &= 0, \end{aligned} \tag{2}$$

where, the operator $[\![\cdot]\!]$ defines the jump in the quantity, namely the difference between its values at $F = 0^+$ and $F = 0^-$. The constant flame speed hypothesis is expressed as

$$S_f = S_L, \tag{3}$$

where S_L is the laminar flame speed, i.e., the speed of a planar adiabatic flame.

The problem depends on two parameters: the flame speed S_L, representing the rate of reactant consumption and the unburned-to-burned density ratio $\sigma \equiv \rho_u/\rho_b$, or equivalently the burned-to-unburned temperature ratio T_b/T_u, representing the extent of heat released by the chemical reactions (the subscripts $_u$ and $_b$ stand for unburned/burned respectively). For the exothermic reactions occuring in combustion studies, $\sigma > 1$.

2.1. Linear stability analysis of a planar flame

The basic state corresponds to a planar adiabatic flame that propagates (along the negative x-axis) at a speed S_L into a quiescent mixture. It is convenient to refer to a coordinate system attached to the flame front assumed located at $x = 0$. In this frame, the problem is steady and the flow field satisfying (1), (3) is given by

$$u = \begin{cases} S_L \\ \sigma S_L \end{cases}, \qquad p = p_0 - \begin{cases} 0 & \text{for } x < 0 \\ (\sigma - 1)\rho_u S_L^2 & \text{for } x > 0, \end{cases} \tag{4}$$

where p_0 is the ambient pressure. Introducing disturbances, denoted by primes, all variables are expressed in the form

$$u = \bar{u}(x) + u'(x, y, t), \qquad v = v'(x, y, t), \qquad p = \bar{p}(x) + p'(x, y, t)$$

where, the 'overline' represents the steady, basic state (4). The perturbed flame front is described by $x = f'(y, t)$. For simplicity we have restricted attention to planar (i.e., two-dimensional) flows. For small disturbances, the Euler equations (1) linearized about the basic state reduce to

$$\frac{\partial u'}{\partial x} + \frac{\partial v'}{\partial y} = 0,$$
$$\rho\frac{\partial u'}{\partial t} + \rho_u S_L \frac{\partial u'}{\partial x} = -\frac{\partial p'}{\partial x},$$
$$\rho\frac{\partial v'}{\partial t} + \rho_u S_L \frac{\partial v'}{\partial x} = -\frac{\partial p'}{\partial y} \tag{5}$$

and must be solved subject to

$$[\![u']\!] = 0, \qquad [\![v']\!] = -(\sigma - 1)S_L\frac{\partial f'}{\partial y}, \qquad [\![p']\!] = 0 \tag{6}$$

across $x = 0$, obtained from the RH relationships (2), with

$$\frac{\partial f'}{\partial t} = u' \qquad \text{at } x = 0 \tag{7}$$

resulting from the flame speed relation (3).

Let the perturbed flame be described by $f' = A\,\mathrm{e}^{\mathrm{i}ky+\omega t}$ where A is the amplitude, k the wavenumber and ω the growth rate and, similarly, express all flow properties in the form

$$u' = U(x)\,\mathrm{e}^{\mathrm{i}ky+\omega t}, \quad v' = V(x)\,\mathrm{e}^{\mathrm{i}ky+\omega t}, \quad p' = P(x)\,\mathrm{e}^{\mathrm{i}ky+\omega t},$$

the problem reduces to the following eigenvalue problem

$$\frac{\mathrm{d}^2P}{\mathrm{d}x^2} - k^2P = 0,$$
$$\rho\omega U + (\rho_u S_L)\frac{\mathrm{d}U}{\mathrm{d}x} = -\frac{\mathrm{d}P}{\mathrm{d}x},$$
$$\frac{\mathrm{d}U}{\mathrm{d}x} + \mathrm{i}kV = 0 \tag{8}$$

$$[\![U]\!] = 0, \quad [\![V]\!] = -\mathrm{i}k(\sigma - 1)S_L A, \quad [\![P]\!] = 0, \quad U(0) = \omega A \tag{9}$$

for the determination of $\omega = \omega(\sigma, S_L)$. It is clear, based on dimensional analysis, that $\omega = \omega_{\mathrm{DL}}(\sigma)S_L k$ such that only the coefficient ω_{DL} and, in particular, the sign of its real part is of interest and remains to be determined.

It is instructive to examine first the special limit of 'weak thermal expansion', namely $\epsilon \equiv \sigma - 1 \ll 1$. Since the discontinuity in velocity across the flame is small, the growth rate is equally small which justifies writing $U = \epsilon\tilde{U}$, $V = \epsilon\tilde{V}$, $P = \epsilon\tilde{P}$, $\omega = \epsilon\tilde{\omega}$. As a result, the first term on the lhs of the second equation in (8) is neglected as a consequence of being $\mathcal{O}(\epsilon^2)$. The solution is

$$\frac{\tilde{U}}{S_L} = \begin{cases} C_1\mathrm{e}^{kx} \\ C_2\mathrm{e}^{-kx} \end{cases}, \qquad \frac{\tilde{V}}{S_L} = \begin{cases} \mathrm{i}C_1\mathrm{e}^{kx} \\ -\mathrm{i}C_2\mathrm{e}^{-kx} \end{cases}, \qquad \frac{\tilde{P}}{\rho_u S_L^2} = \begin{cases} -C_1\mathrm{e}^{kx} & (x < 0) \\ -C_2\mathrm{e}^{-kx} & (x > 0) \end{cases}$$

with $C_1 = C_2 = \frac{1}{2}kA$ and $\tilde{\omega} = \frac{1}{2}kS_L$. Hence $\omega \sim \frac{1}{2}(\sigma - 1)kS_L$ is positive for all k, and the planar flame is unstable to disturbances of all wavelengths.

Note that although the vorticity is (to this order) zero everywhere, the discontinuity in the transverse velocity along $x = 0$ implies that vorticity is being concentrated along the sheet. The disturbed flame is therefore equivalent to a flat vortex sheet along the mean position $x = 0$, as shown in figure 2. The sense of rotation, dictated by (6), is as shown in the figure; counterclockwise when the slope of $f'(y)$ is positive and clockwise when the slope of $f'(y)$ is negative. The concentrated vorticity through the Biot–Savart law induces an axial velocity u'

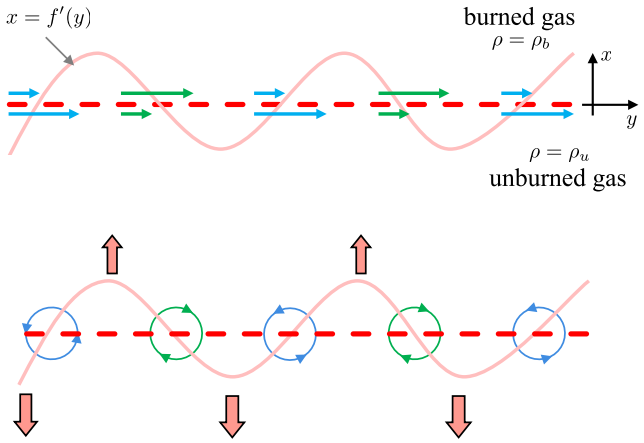

Figure 2. The perturbed planar flame, equivalent to a vortex-sheet.

which, according to (7) convects segments of the flame intruding towards the burned gas further downstream and segments intruding towards the unburned gas further upstream, thus amplifying the initially disturbed flame. A slightly different, but equivalent interpretation of the instability can be found in Williams (1985).

The physical interpretation for the instability just outlined could presumably be extended to the more realistic case of $\sigma - 1 = \mathcal{O}(1)$, except that now there will be vorticity distributed in the burned gas as well, and its role on stability is not clear a-priori. We will show below that the vorticity created at the flame front is convected in the burned gas region along streamlines and does not affect the instability conclusion. Indeed, the larger heat release and the associated gas expansion cause an increase in the growth rate ω and an enhancement of the instability.

For finite values of thermal expansion, the solution of the eigenvalue problem (8), (9) can be easily obtained. One finds

$$\begin{aligned}
\frac{U}{S_L} &= \begin{cases} C_1\, \mathrm{e}^{kx} & (x<0) \\ C_2\, \mathrm{e}^{-kx} + C_3 \mathrm{e}^{-(\omega/\sigma S_L)x} & (x>0), \end{cases} \\
\frac{V}{S_L} &= \begin{cases} \mathrm{i}C_1\, \mathrm{e}^{kx} & (x<0) \\ -\mathrm{i}C_2\, \mathrm{e}^{-kx} - \mathrm{i}C_3 \dfrac{\omega}{\sigma k S_L} \mathrm{e}^{-(\omega/\sigma S_L)\,x} & (x>0), \end{cases} \\
\frac{P}{\rho_u S_L^2} &= \begin{cases} -C_1\left(1 + \dfrac{\omega}{kS_L}\right) \mathrm{e}^{kx} & (x<0) \\ -C_2\left(1 - \dfrac{\omega}{\sigma k S_L}\right) \mathrm{e}^{-kx} & (x>0), \end{cases}
\end{aligned} \tag{10}$$

where the terms multiplying C_3 clearly accounts for the vorticity in the burned gas region. The conditions (9) then yield

$$\begin{pmatrix} 0 & 1 & -1 & -1 \\ -kS_L(\sigma-1) & 1 & 1 & \dfrac{\omega}{\sigma k S_L} \\ 0 & 1 + \dfrac{\omega}{kS_L} & \dfrac{\omega}{\sigma k S_L} - 1 & 0 \\ -\omega & 1 & 0 & 0 \end{pmatrix} \begin{pmatrix} A \\ C_1 \\ C_2 \\ C_3 \end{pmatrix} = 0.$$

The solvability condition yields the dispersion relation

$$(\sigma + 1)\omega^2 + 2\sigma k S_L \omega - \sigma(\sigma - 1)k^2 S_L^2 = 0. \tag{11}$$

For $\sigma > 1$, one of the two roots is always positive and given by

$$\omega = \underbrace{\frac{1}{\sigma + 1}[\sqrt{\sigma^3 + \sigma^2 - \sigma} - \sigma]}_{\omega_{\rm DL}} S_L k. \tag{12}$$

This result can be easily extended to three-dimensions in which case the wavenumber $k = (k_y^2 + k_z^2)^{1/2}$, where k_y and k_z are the wavenumbers in the y and z directions, respectively.

Thus, planar flames are *unconditionally unstable*. Disturbances of all wavelength are amplified and the amplification rate increases with increasing σ. Moreover, the growth rate increases when increasing k, implying that the short waves grow faster than the long waves. This is the celebrated hydrodynamic or DL instability.

2.2. The Markstein model

The DL conclusion seems contradictory to observations, which prompted investigators to seek improvements of the model to reconcile between theoretical predictions and laboratory observations. The most notable results are due to Markstein (1951) who also treated the flame as a surface of discontinuity, but assumed a dependence of the flame speed on the local curvature of the flame front through a phenomenological constant assumed to be proportional to the flame thickness; see also Markstein's monograph (Markstein 1964). The only modification to the DL model is therefore the relation

$$S_f = S_L - \mathcal{L}\kappa \tag{13}$$

replacing (3), where $\kappa = -\nabla \cdot \mathbf{n}$ is the local curvature of the flame surface. The coefficient $\mathcal{L}$, in units of length is nowadays referred to as the Markstein length. The linear stability analysis of the planar solution yields the dispersion relation

$$(\sigma + 1)\,\omega^2 + 2(1 + \mathcal{L}k)\sigma k S_L \omega - (\sigma - 1 - 2\sigma\mathcal{L}k)\sigma k^2 S_L^2 = 0, \tag{14}$$

with the DL growth rate recovered when $\mathcal{L} = 0$. When $\mathcal{L} < 0$ the planar flame remains unconditionally unstable, with disturbances growing at a rate faster than the DL growth rate $\omega_{\rm DL}$. When $\mathcal{L} > 0$, on the other hand, the short wavelength disturbances are damped and only disturbances with wavelength $\lambda \equiv 2\pi/k > \lambda_c$are amplified. The critical wavenumber is $\lambda_c = 4\pi\sigma\mathcal{L}/(\sigma - 1)$. Hence, in domains of lateral size $L < \lambda_c$ the planar flame is stable. The stabilization mechanism is readily understood; the enhanced flame speed at the crests, where $\kappa < 0$, and the reduced speed at the troughs, where $\kappa > 0$, tend to dampen the amplitude of the corrugations.

2.3. Comments

The aforementioned analyses raise a number of questions.

- Although the flame zone associated with the region where heat conduction, species diffusion, viscous dissipation and chemical reactions occur is thin, it nevertheless has a finite thickness. Treating the flame as a discontinuity can be justified for perturbations of large wavelength, but the assumption fails when the perturbation's wavelength becomes comparable to the flame thickness, i.e., for large values of k. One then expects that the

physicochemical processes occurring inside the flame zone have some influence on its stability. Markstein's suggestion has clearly addressed this issue, but the dependence of the Markstein length on the mixture properties remains unknown and must be determined.

- The assumptions that the flame speed is constant along the flame surface, as assumed by Darrieus (1938) and Landau (1944), or depends solely on the flame curvature as hypothesized by Markstein (1964), need to be reexamined. One may anticipate that the flame speed also depends on nonuniformities in the underlying flow field, an idea first explored by Eckhaus (1961). Preferably, such a relation needs to be derived from physical first principles.
- Even when the diffusion processes occurring inside the flame zone provide stabilization of the short wavelength disturbances, the long waves pertinent to large-scale flames are amplified by hydrodynamic effects. The question then is whether the growth rate eventually saturates by nonlinear effects, not accounted for in the linear theory, and what is the ultimate conformation adopted by the flame surface.
- Finally, of interest is whether the DL instability, ubiquitous under laminar flow conditions, has an influence on turbulent flames and under what conditions.

3. Hydrodynamic theory—multi-scale analysis

An appropriate mathematical framework for the description of time-dependent, multi-dimensional flames is the *hydrodynamic theory* developed by Matalon and Matkowsky (1982) using a multi-scale approach, and extended by Matalon *et al* (2003) to account for temperature-dependent transport, differential/preferential diffusion and effects due to stoichiometry. The asymptotic derivation exploits the disparity in length scales associated with the hydrodynamic field, the flame zone where heat and mass transport occur and the reaction zone where the chemical reactions take place. If L is a characteristic length associated with the hydrodynamic field and $l_f = \mathcal{D}_{\rm th}/S_{\rm L}$ a representative diffusion length, where $\mathcal{D}_{\rm th}$ is the thermal diffusivity of the fresh mixture, the ratio $\delta \equiv l_f/L$ is a measure of the flame thickness. Chemical reaction occurs in a thin region within the flame on the order of l_f/β where $\beta \gg 1$ is the activation energy parameter, or Zel'dovich number, given by $\beta = E(T_b - T_u)/\mathcal{R}T_b^2$ with E is the overall activation energy and $\mathcal{R}$ the gas constant. A schematic of the flame structure is given in figure 3.

The flame, consisting of the region where diffusion processes and chemical reaction occur, is relatively thin (typically a fraction of a millimeter) and shrinks to a surface when $\delta \to 0$. Viewed on the hydrodynamic length scale the entire flame may therefore be represented as a surface that separates the fresh mixture from the burned gas, as envisaged by Darrieus and Landau. However, contrary to their structureless model, the balance equations for the energy of the mixture and for the mass fractions of the fuel and oxidizer are integrated across the flame zone to derive an expression for the flame speed. Since for thin flames the integration is primarily carried out along the normal to the flame surface, the equations to leading order are quasi-steady and quasi-one dimensional and can be integrated exactly in the limit of large activation energy ($\beta \to \infty$). To include effects due to the finite thickness of the flame, the derivation must proceed to $\mathcal{O}(\delta)$. Asymptotic matching then provides expressions relating the flow properties on the burned and unburned sides of the flame, as well as an expression for the flame speed.

The flow field on either side of the flame front is governed by the incompressible Navier–Stokes equations

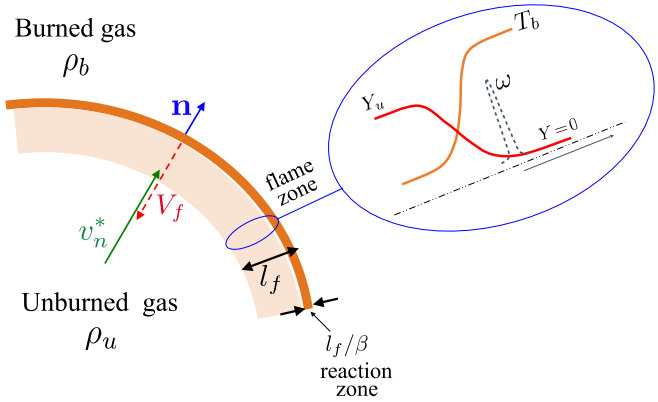

Figure 3. The structure of a curved premixed flame. The inset shows the structure of the flame zone, where the temperature rises from the unburned value T_u to the burned temperature T_b and where the fuel (the deficient component in the mixture) diffuses from its value Y_u in the fresh mixture to $Y = 0$ in the reaction zone. The reaction rate ω is practically a delta-function centered near T_b.

$$\nabla \cdot \mathbf{v} = 0, \qquad \rho\left(\frac{\partial \mathbf{v}}{\partial t} + (\mathbf{v} \cdot \nabla)\mathbf{v}\right) = -\nabla p + \nabla \cdot (2\mu \mathbf{E}), \tag{15}$$

where $\mathbf{E}$ is the strain rate tensor and μ the viscosity of the mixture, which assumes different values in the unburned and burned regions. Consistent will all other diffusion processes, the viscous term in (15) is an $\mathcal{O}(\delta)$ correction term. The transport coefficients μ, λ/c_p, $\rho\mathcal{D}_F$, $\rho\mathcal{D}_O$, where λ and c_p are the thermal conductivity and specific heat of the mixture and $\mathcal{D}_F$, $\mathcal{D}_O$ the molecular diffusivities of the fuel and oxidizer, are assumed to have the same temperature dependence implying that their ratios, corresponding to the fuel and oxidizer Lewis numbers and the Prandtl number, given respectively by

$$\mathrm{Le}_{_F} = \frac{\lambda/c_p}{\rho\mathcal{D}_F}, \quad \mathrm{Le}_{_O} = \frac{\lambda/c_p}{\rho\mathcal{D}_O}, \quad \mathrm{Pr} = \frac{\mu}{\lambda/c_p},$$

are constants. (There should be no confusion with the notation of λ here being the conductivity of the gaseous mixture, because it is only used in the description of the hydrodynamic model.)

The flame speed is given by

$$S_f = S_L - \mathcal{L}\mathbb{K}, \tag{16}$$

where $\mathbb{K}$ is the flame stretch rate, which is a measure of the deformation of the flame front resulting from its motion and from non-uniformities in the underlying flow field. An invariant expression for flame stretch given by Matalon (1983) takes the form

$$\mathbb{K} = -V_f\,\kappa - \mathbf{n} \cdot \nabla \times (\mathbf{v}^* \times \mathbf{n}), \tag{17}$$

where the first term on the rhs corresponds to surface dilatation, resulting from the motion of a segment of the flame surface of curvature κ, and the second term to surface extension resulting from the velocity gradient along the flame surface[2]. Flame stretch can be also

[2] Two canonical examples illustrating each of the two terms in (17) are, respectively, (i) a spherically expanding flame where the flow is radial and $\mathbb{K} = 2\dot{R}/R$, with R the flame radius and $\dot{R}$ the propagation speed; and (ii) a flat flame in the straining field of a stagnation-point flow, which is being stretched by the transverse velocity gradient equal to the strain rate.

expressed in the form $\mathbb{K} = \kappa S_L - \mathbf{n}\cdot\mathbf{E}\cdot\mathbf{n}$, where the first term contains all contributions associated with the curvature κ and the second term is the hydrodynamic strain experienced by the flame. When relating this expression to (17), the constraint $\nabla\cdot\mathbf{v} = 0$ is imposed, consistent with (15). The jump relations across the flame are generalized RH relations that include $\mathcal{O}(\delta)$ corrections accounting for accumulation and/or transverse fluxes inside the flame zone; their explicit form can be found in Matalon *et al* (2003). The coefficient $\mathcal{L}$ in the flame speed relation (16), which is being appropriately referred to as the Markstein length, is given by

$$\mathcal{L} = \left\{ \frac{\sigma}{\sigma-1}\int_1^\sigma \frac{\tilde\lambda(x)}{x}\,\mathrm{d}x + \frac{\beta(\mathrm{Le}_{\mathrm{eff}}-1)}{2(\sigma-1)}\int_1^\sigma \frac{\tilde\lambda(x)}{x}\ln\left(\frac{\sigma-1}{x-1}\right)\mathrm{d}x \right\} l_f. \tag{18}$$

Note that equation (16) not only generalizes Markstein's hypothesis by including a dependence on the strain rate, absent in the Markstein model (13), but also determines the coefficient $\mathcal{L}$ from physical first principles.

The Markstein length is proportional to the flame thickness l_f and depends on (i) the thermal expansion coefficient σ, or the extent of heat released during combustion, (ii) the common temperature dependence of the diffusion coefficients $\tilde\lambda(T)$, scaled by its value in the unburned gas, (iii) the overall activation energy of the chemical reaction, or the Zel'dovich number β, and (iv) the effective Lewis number $\mathrm{Le}_{\mathrm{eff}}$ of the mixture. The effective Lewis number $\mathrm{Le}_{\mathrm{eff}}$ is a weighted average of the individual Lewis numbers, Le_F and Le_O, respectively. For unitary reaction orders with respect to each of the two reactants, the effective Lewis number is expressed in the form

$$\mathrm{Le}_{\mathrm{eff}} = \begin{cases} \dfrac{\mathrm{Le}_O + \mathcal{A}\,\mathrm{Le}_F}{1+\mathcal{A}} & \text{lean mixture } (\phi<1) \\ \dfrac{\mathrm{Le}_F + \mathcal{A}\,\mathrm{Le}_O}{1+\mathcal{A}} & \text{rich mixture } (\phi>1), \end{cases}$$

where ϕ is the mixture equivalence ratio, and

$$\mathcal{A} = \begin{cases} 1+\beta(\phi^{-1}-1) & (\phi<1) \\ 1+\beta(\phi-1) & (\phi>1) \end{cases}$$

measures the deviation from stoichiometry. The more general expression for arbitrary reaction orders can be found in Matalon *et al* (2003). For a stoichiometric mixture ($\phi = 1$), the effective Lewis number is the average of the individual Lewis numbers of the two reactants. For an off-stoichiometric mixture the deficient component is more heavily weighted such that for very lean/rich mixtures ($\mathcal{A} \gg 1$) the effective Lewis number is practically that of the fuel/oxidizer, respectively. figure 4 shows the variations of $\mathrm{Le}_{\mathrm{eff}}$ with equivalence ratio for two mixtures. Hydrogen, which is a light fuel diffuses relatively fast such that $\mathrm{Le}_{\mathrm{eff}}$ for a lean mixture is smaller than unity. Propane, which is a heavy fuel diffuses slowly and $\mathrm{Le}_{\mathrm{eff}}$ for lean mixtures is larger than unity. In rich mixtures, $\mathrm{Le}_{\mathrm{eff}}$ depends primarily on the mixture composition and the diffusivity of the oxidizer. Accordingly, $\mathrm{Le}_{\mathrm{eff}}$ for a hydrogen–air mixture is a monotonically increasing function of equivalence ratio, whereas for hydrocarbon-air mixtures (with the possible exception of methane) it is a monotonically decreasing function of equivalence ratio.

The Markstein length $\mathcal{L}$ can, therefore, be positive or negative depending on the mixture composition, or specifically on $\mathrm{Le}_{\mathrm{eff}}$. It is generally positive for rich hydrogen–air and lean hydrocarbon-air mixtures and negative for lean hydrogen–air and rich hydrocarbon–air mixtures. In an experimental setting, changes in $\mathcal{L}$ are accommodated by varying the fuel type

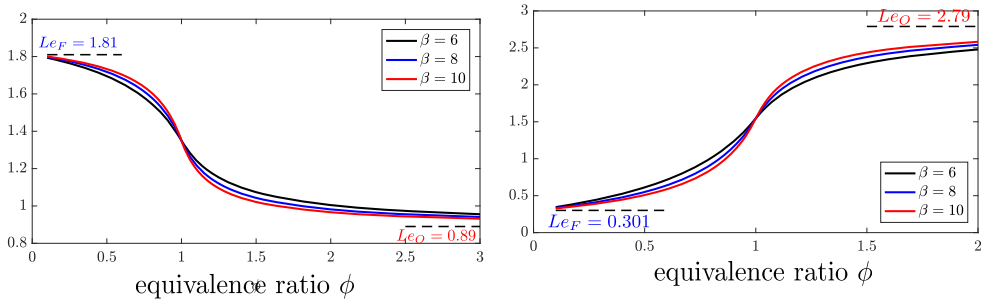

(a) Propane-air mixture (b) Hydrogen-air mixture

Figure 4. The effective Lewis number $\mathrm{Le}_{\mathrm{eff}}$ as a function of equivalence ratio, for various values of the Zel'dovich number β.

and mixture composition, or by changing the system's pressure, which affects the flame thickness.

In summary, the hydrodynamic theory extends the DL model by accounting for all the diffusion processes occurring inside the flame zone as a perturbation to the governing equations, the jump relations across the flame, and the flame speed relation. The additional parameters appearing in the formulation include the viscosities of the burned/unburned gas and the Markstein length $\mathcal{L}$ that mimics all diffusion properties of the mixture.

3.1. Linear stability results

Reexamining the stability of a planar flame within the context of the hydrodynamic theory leads to the following dispersion relation

$$\omega = \omega_{\mathrm{DL}} S_L k - l_f [B_1 + \beta(\mathrm{Le}_{\mathrm{eff}} - 1)B_2 + \mathrm{Pr}\, B_3] S_L k^2 + \cdots, \tag{19}$$

where B_1, B_2 and B_3 are all positive and depend only on σ. They are given by

$$B_1 = \frac{\sigma/2}{\sigma + (\sigma+1)\omega_{\mathrm{DL}}}\left\{\frac{\sigma(2\omega_{\mathrm{DL}} + \sigma + 1)}{\sigma - 1}\int_1^\sigma \frac{\tilde{\lambda}(x)}{x}\mathrm{d}x + \int_1^\sigma \tilde{\lambda}(x)\mathrm{d}x\right\},$$

$$B_2 = \frac{\sigma/2}{\sigma + (\sigma+1)\omega_{\mathrm{DL}}}\left\{\frac{(1+\omega_{\mathrm{DL}})(\sigma+\omega_{\mathrm{DL}})}{\sigma - 1}\int_1^\sigma \ln\left(\frac{\sigma-1}{x-1}\right)\frac{\tilde{\lambda}(x)}{x}\mathrm{d}x\right\},$$

$$B_3 = \frac{\sigma}{\sigma + (\sigma+1)\omega_{\mathrm{DL}}}\left\{(\sigma-1)\tilde{\lambda}(\sigma) - \int_1^\sigma \tilde{\lambda}(x)\mathrm{d}x\right\}.$$

Since typically $\tilde{\lambda} \sim (T/T_u)^a$ with $a \approx 0.7$, the two extreme cases $a = 0$, 1 corresponding to constant transport and $\tilde{\lambda} \sim T$, are of special interest. Simplified expressions for B_1, B_2, B_3 for these two cases are listed in the appendix.

The growth rate (19) shows that the correction to the DL result, proportional to the flame thickness, consists of three terms representing respectively the influences of thermal, molecular and viscous diffusion on stability. Thermal diffusion, which tends to smooth out temperature differences, always has a stabilizing influence. Due to the large change in viscosity across the flame, viscous diffusion also has a stabilizing influence. (This effect is absent when the viscosity is assumed constant throughout the combustion field, in which case $B_3 = 0$ as noted in the appendix.) The effect of molecular diffusion, on the other hand

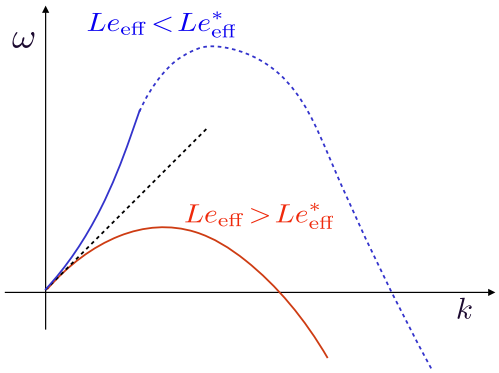

Figure 5. The growth rate ω as a function of the wavenumber k, illustrating the distinction between purely hydrodynamic ($\mathrm{Le}_{\rm eff} > \mathrm{Le}^*_{\rm eff}$) and thermo-diffusive ($\mathrm{Le}_{\rm eff} < \mathrm{Le}^*_{\rm eff}$) instabilities. The dashed part of the curve for $\mathrm{Le}_{\rm eff} < \mathrm{Le}^*_{\rm eff}$ has been extended in anticipation of short wave stabilization obtained at higher orders.

depends on the mixture composition, or the effective Lewis number of the mixture. It has a stabilizing influence when $\mathrm{Le}_{\rm eff} > 1$ and a destabilizing influence, otherwise.

To ensure stabilization of the short wavelength disturbances, the overall contribution of diffusion must be positive, implying that $\mathrm{Le}_{\rm eff}$ must exceed a critical value, $\mathrm{Le}^*_{\rm eff}$ found to be slightly less than unity; see figure 5. For $\mathrm{Le}_{\rm eff} > \mathrm{Le}^*_{\rm eff}$, stable flames may result when the long wavelength disturbances are excluded due to the transverse size of the domain within which the flame is propagating (or damped by other effects, such as gravity, not discussed here). The instability, which will be predominantly observed in large-scale flames is evidently the *hydrodynamic instability*. For $\mathrm{Le}_{\rm eff} < \mathrm{Le}^*_{\rm eff}$ diffusion effects act to further destabilize the flame, a limit referred here as the *thermo-diffusive instability*. The implication that in this limit the competing effects of mass and thermal diffusion play an equally important role on the instability is based on the results of Barenblatt *et al* (1962) and Sivashinsky (1977a) obtained when the hydrodynamic disturbances have been filtered out by adopting a constant-density approximation. Stabilization of the short wavelength will presumably arise in this case from higher order terms, as implied from numerical simulations (Altantzis *et al* 2012), but these have not been analytically computed (see the dashed curve in figure 5). Clearly, in this regime hydrodynamic and thermo-diffusive effects act in synergy, unlike when $\mathrm{Le}_{\rm eff} > \mathrm{Le}^*_{\rm eff}$ where the instability is purely hydrodynamic. Since $\omega \sim k$ when $k \to 0$, the distinction between the thermo-diffusive and hydrodynamic instabilities may be associated with the existence, or lack of an inflection point in the functional dependence of the growth rate ω on the wavenumber k, a criterion verified in the simulations reported by Altantzis *et al* (2012).

It should be emphasized that the often expressed statement that the hydrodynamic and thermo-diffusive instabilities result in rich/lean hydrogen–air, or lean/rich hydrocarbon–air mixtures is a gross characterization of this observation. According to the theory, the transition occurs at $\mathrm{Le}_{\rm eff} = \mathrm{Le}^*_{\rm eff}$ which, for hydrogen–air flames corresponds to $\phi \approx 0.75$. And, indeed, based on the inflection-point criterion, further substantiated by the nonlinear flame development, numerical simulations of hydrogen–air flames (Frouzakis *et al* 2015) predicts that the transition from hydrodynamic to thermo-diffusive instability occurs at a value of equivalence ratio slightly larger than $\phi = 0.75$.

3.2. Relation to the Markstein model

It was noted by Creta and Matalon (2011) that, when reconsidering the Markstein model discussed in section 2.2 but with the correct expression (16) for the flame speed that includes the effects of both curvature and strain, the dispersion relation (14) is replaced by

$$[(\sigma+1)+(\sigma-1)\mathcal{L}k]\,\omega^2 + 2\sigma(1+\sigma\mathcal{L}k)kS_L\omega \\ -[(\sigma-1)-2\sigma\mathcal{L}k-(\sigma-1)\mathcal{L}k]\sigma k^2S_L^2 = 0. \tag{20}$$

As before, the planar flame is unstable when $\mathcal{L}<0$. For $\mathcal{L}>0$, however, only disturbances with wavelength $\lambda>\lambda_c$ are amplified, with the critical wavenumber given by $\lambda_c=2\pi(3\sigma-1)\mathcal{L}/(\sigma-1)$, compared to $4\pi\sigma\mathcal{L}/(\sigma-1)$ in the absence of strain. Hence the inclusion of straining effects reduces the interval of unstable modes, adding a stabilizing effect on the short wave disturbances. When $\sigma-1\to 0$, the effects of straining disappear and (20) reduces to (14) implying that straining effects are a direct consequence of thermal expansion.

Implicit in the Markstein model is the assumption that $\mathcal{L}k\ll 1$. This suggests expanding the growth rate resulting from the dispersion relation (20) accordingly. The result

$$\omega\sim\omega_{\rm DL}S_Lk-\mathcal{L}\,\frac{\sigma(1+\omega_{\rm DL})(\sigma+\omega_{\rm DL})}{\sigma+(\sigma+1)\omega_{\rm DL}}S_Lk^2+\cdots$$

is similar in form to the rigorous asymptotic expression (19). Since variations in Markstein length are primarily associated with variations in the effective Lewis number, the latter may be also expressed in the form

$$\omega\sim\omega_{\rm DL}S_Lk-(\mathcal{L}-\mathcal{L}_c)\,\frac{\sigma(1+\omega_{\rm DL})(\sigma+\omega_{\rm DL})}{\sigma+(\sigma+1)\omega_{\rm DL}}S_Lk^2+\cdots,$$

where $\mathcal{L}_c$ is a function of σ and Pr only. For constant transport properties ($\tilde\lambda=1$), for example, it depends only on σ since $B_3=0$ (see appendix), and is given

$$\mathcal{L}_c=\left\{\frac{\sigma\ln\sigma}{\sigma-1}-\frac{(\sigma+1+2\omega_{\rm DL})\frac{\sigma\ln\sigma}{\sigma-1}+\sigma-1}{2(1+\omega_{\rm DL})(\sigma+\omega_{\rm DL})}\right\}l_f.$$

The two expressions are identical except for $\mathcal{L}_c$, which identifies the Markstein length above which diffusion effects have stabilizing influences on the flame dynamics. For the Markstein model, the critical value is $\mathcal{L}_c=0$. This suggests that the $\mathcal{O}(\delta)$ corrections to the RH relations, neglected in the Markstein model, affect only the determination of $\mathcal{L}_c$, but the qualitative prediction of this model remains similar to the predictions of the asymptotic results.

The focus in the discussion below is on nonlinear studies associated with the *hydrodynamic instability*, namely when $\mathrm{Le}_{\rm eff}>\mathrm{Le}^*_{\rm eff}$ or, equivalently $\mathcal{L}>0$.

4. Nonlinear flame development

Insight into the understanding of nonlinear development of hydrodynamically unstable flames has been achieved by examining the problem in the weak thermal expansion limit. This limit is discussed first, followed by numerical results carried out within the context of the hydrodynamic theory, for realistic values of gas expansion.

4.1. Weakly nonlinear analysis; $\sigma-1\ll1$

We consider first the weak thermal expansion limit $\epsilon \equiv \sigma - 1 \ll 1$, in which case the problem simplifies to a single equation that describes the evolution of the flame front. The equation, known as the Michelson–Sivashinsky (MS) equation, was derived by Sivashinsky (1977b) and the first numerical integration was provided by Michelson and Sivashinsky (1977). Since in this limit the DL growth rate $\omega_{\text{DL}} \sim \sigma - 1$, the evolution occurs on the slow time $\tau = \epsilon t$, with the perturbed front (in a coordinate system attached to the flame) expressed as $x = \epsilon\, \varphi(y, \tau)$. If perturbations in the velocity and pressure fields are $\mathcal{O}(\epsilon^2)$, the flame speed relation (16) simplifies to

$$\frac{\partial \varphi}{\partial \tau} + \tfrac{1}{2} S_L \left(\frac{\partial \varphi}{\partial y}\right)^2 - \frac{\mathcal{L} S_L}{\epsilon} \frac{\partial^2 \varphi}{\partial y^2} - \tilde{u}^* = o(\epsilon^2), \tag{21}$$

where $\tilde{u}^*(y, \tau)$ is the perturbation of the axial velocity component, evaluated at the flame front. The first two terms are the simplification of the propagation speed V_f for weakly curved flames. The third term represents the effect of curvature and is the only contribution of stretch that remains in the present context; for the weakly induced flow the effects of strain are $o(\epsilon^2)$. The last term represents the induced velocity due to gas expansion. Correct to $\mathcal{O}(\epsilon^2)$ the density is practically constant, and Euler's equations with the associated RH conditions (5), (6) simplify to

$$\frac{\partial \tilde{u}}{\partial x} + \frac{\partial \tilde{v}}{\partial y} = 0, \qquad \rho_u S_L \frac{\partial \tilde{u}}{\partial x} = -\frac{\partial \tilde{p}}{\partial x}, \qquad \rho_u S_L \frac{\partial \tilde{v}}{\partial x} = -\frac{\partial \tilde{p}}{\partial y},$$

$$[\![\tilde{u}]\!] = 0, \qquad [\![\tilde{v}]\!] = -S_L \frac{\partial \varphi}{\partial y}, \qquad [\![\tilde{p}]\!] = 0.$$

The solution, using Fourier transform in y, yields

$$\tilde{u}^* = \frac{S_L}{2} \cdot \frac{1}{2\pi} \iint_{-\infty}^{\infty} |k|\, \mathrm{e}^{\mathrm{i}k(y-\eta)}\, \varphi(\eta, \tau) \mathrm{d}k\, \mathrm{d}\xi \equiv \frac{S_L}{2} \cdot \mathbb{I}\{\varphi\}$$

and, when substituted in (21), a single nonlinear integro-differential equation results for the determination of φ.

Let L, the transverse domain of integration, be used as a unit of length, S_L as a unit of speed and L/S_L as a unit of time, and let the density be scaled with respect to its value in the unburned gas, the MS equation in dimensionless form,

$$\frac{\partial \varphi}{\partial \tau} + \tfrac{1}{2} \left(\frac{\partial \varphi}{\partial y}\right)^2 - \alpha \frac{\partial^2 \varphi}{\partial y^2} - \tfrac{1}{2} \mathbb{I}\{\varphi\} = 0, \tag{22}$$

depends on a single parameter $\alpha \equiv \mathcal{L}/\epsilon L$ corresponding to a 'scaled' Markstein number. The operator $\mathbb{I}\{\varphi\}$ is a linear, non-local operator which in Fourier space constitutes a multiplication by $|k|$; i.e., $\mathbb{I}\{\cos(kx)\} = |k| \cos(kx)$. It may also be expressed as the Hilbert transform (denoted by $\mathcal{H}$) of the derivative of φ, namely $\mathbb{I}\{\varphi; y\} = -\mathcal{H}\{\varphi_y; y\}$.

The stability of a planar flame, $\varphi = 0$, is readily obtained by examining the linearized form of equation (22). Seeking solutions $\sim \exp(\mathrm{i}ky + \omega\tau)$, the growth rate $\omega = \left(\frac{1}{2} - \alpha k\right)k$ implying stability for $\alpha > (4\pi)^{-1}$, or in domains $L < 4\pi\mathcal{L}/(\sigma - 1)$, in accord with the results of section 2.2.

The nonlinear equation (22) was recognized by Thual *et al* (1985) to correspond to a class of equations for which an infinite number of exact solutions, known as 'pole solutions', exist. The pole solutions consist of a superposition of a finite number of poles. A pole in the

complex plane corresponds in the physical plane to a sharp indentation of the flame surface, pointing towards the burned gas and rounded at its tip, to which we refer loosely as a 'cusp'. The real part of the pole corresponds to the location of the cusp along the flame front and the imaginary part of the pole is a measure of the depth of the cusp, or the amplitude of the flame surface. A distinct set of pole solutions is the 'coalescent pole solutions' for which the poles (or cusps) align themselves vertically and coalesce into a single location. Of particular interest is the family of coalescent pole solutions for which the poles are time-independent. On a finite domain, $0 \leqslant y \leqslant 1$, with periodic boundary conditions the solution takes the form

$$\varphi = -U\tau + \Phi(y) \tag{23}$$

and corresponds to a steadily propagating pattern; namely a pattern that propagates at a constant speed U without change in shape. The propagation speed is directly obtained from (22) by taking the spatial average, namely

$$U = \frac{1}{2}\int_0^1 \left(\frac{\mathrm{d}\Phi}{\mathrm{d}y}\right)^2 \mathrm{d}y,$$

so that the fractional increase in propagation speed is equal to the fractional increase in surface area of the flame front.

The members of the family of steady coalescent pole solutions are distinguished by the number N of pairs of complex conjugate poles that contribute to the solution, such that an N-pole solution Φ_N, with $N = 0, 1, \ldots$ is a solution made up of N pairs of poles. The zero-pole solution corresponds to the trivial solution $\Phi = 0$, or the planar flame front. The N-pole solution, with $N \geqslant 1$, takes the form

$$\Phi_N(y) = -2\alpha \sum_{n=1}^{N} \ln \tfrac{1}{2}[\cosh(x_n) - \cos(2\pi y - y_c)],$$

where y_c is the location of the cusp (the common real part of the poles) and the values x_n (the imaginary parts of the poles) for $n = 1, \ldots, N$ are the solutions of N-nonlinear algebraic equations

$$\coth x_n + \sum_{\substack{l=1 \\ l\neq n}}^{N} \coth\left[\tfrac{1}{2}(x_n - x_l)\right] + \coth\left[\tfrac{1}{2}(x_n + x_l)\right] = \frac{1}{4\pi\alpha}.$$

The propagation speed of the N-pole solution is given

$$U_N = 2\pi\alpha N(1 - 4\pi\alpha N).$$

The larger the value of N, the larger the peak (or amplitude) of the flame front as shown in figure 6(a), and the faster the propagation speed.

To discuss the properties of the pole solutions it is convenient to introduce the reciprocal of the Markstein number, $\gamma = (2\pi\alpha)^{-1}$, which is directly proportional to the transverse size of the domain of integration. For a given γ, there is an upper bound on the number of poles that a member in the family of steady coalescent pole solutions can possess, i.e., $N \leqslant N_0(\gamma)$, where

$$N_0 = \begin{cases} \mathrm{Int}\left[\frac{\gamma}{4} + \frac{1}{2}\right] & \text{if } \frac{\gamma}{4} + \frac{1}{2} \text{ is not an integer} \\ \mathrm{Int}\left[\frac{\gamma}{4} - \frac{1}{2}\right] & \text{if } \frac{\gamma}{4} + \frac{1}{2} \text{ is an integer} \end{cases}$$

and $\mathrm{Int}(z)$ denotes the greatest integer less than or equal to the real number z. The trivial solution $\Phi = 0$, or the zero-pole solution, exists for all $\gamma > 0$. At $\gamma = 2$ the one-pole solution

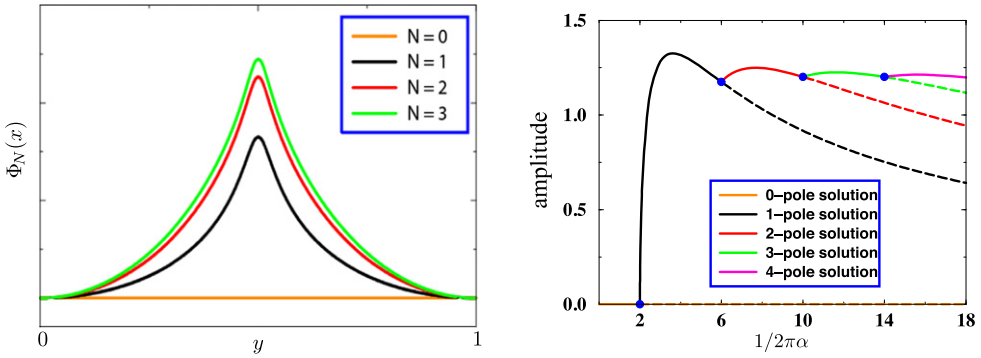

(a) Flame structure (b) Amplitude

Figure 6. The structure of the flame front and its amplitude (solid/dashed curves correspond to stable/unstable solutions) as a function of the inverse Markstein number $(2\pi\alpha)^{-1}$.

emerges as a new bifurcating solution; at $\gamma = 6$ the two-pole solution branches out from the 1-pole solution and, in general, the N-pole solution bifurcates from the $(N-1)$-pole solution at $\gamma = 2(2N-1)$.

Of greatest importance is the stability of the pole solutions established by Vaynblat and Matalon (2000a, 2000b), which show that for any value of γ there exists *one and only one stable* coalescent pole solution, and that the stable solution corresponds to the one with the maximum number of poles $N_0(\gamma)$. Accordingly, the planar flame front, or zero-pole solution, is the stable solution for $0 < \gamma < 2$; the one-pole solution is the stable solution for $2 < \gamma < 6$; the two-pole solution is the stable solution for $6 < \gamma < 10$; etc, so that, in general, the $(N-1)$-pole solution loses stability in favor of the N-pole solution. The amplitude of the flame profiles for increasing values of γ is shown in figure 6(b), where the stable/unstable solutions are shown by solid/dashed curves respectively. Hence, as γ increases (or α decreases), the stable equilibrium states of the MS equation undergo a cascade of supercritical bifurcations corresponding to structures of sharper and sharper cusps that propagate at a speed that increases with increasing γ and asymptotes to a constant value $U_\infty = 1/8$. As $\gamma \to \infty$ (or $\alpha \to 0$), the shape of the solution tends to a genuine cusp, but of finite amplitude, that propagates at a speed U_∞.

The aforementioned results imply that when starting with arbitrary initial conditions, the solution of the MS equation for given α converges to the corresponding stable pole solution. Numerical simulations (Michelson and Sivashinsky 1977, Gutman and Sivashinsky 1990, Rastigejev and Matalon 2006) show that the short wavelength corrugations introduced through the initial conditions merge, forming bigger cells as time progresses that eventually coalesce into a single-peak structure filling up the entire interval. We note parenthetically that the solution for small values of α is quite sensitive to noise and reaching the stable solution numerically requires a fine spatial resolution along with a very small time-step (Rahibe *et al* 1996, Rastigejev and Matalon 2006).

The generalization of the MS equation to a two-dimensional flame surface $\varphi(y, z, \tau)$ is straightforward. The MS equation (in dimensionless form) now reads

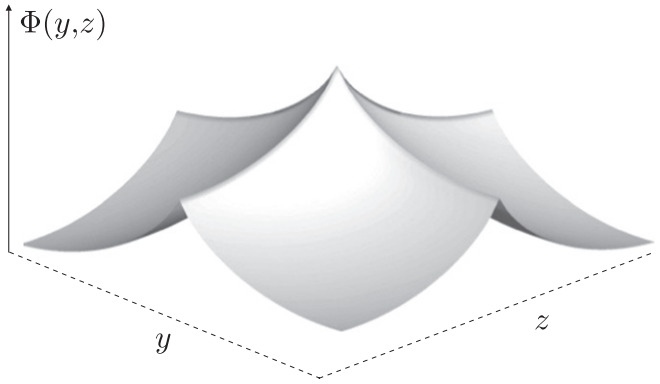

Figure 7. Analytical pole solution of the two-dimensional MS equation, computed for $\alpha = 0.01$.

$$\frac{\partial \varphi}{\partial \tau} + \tfrac{1}{2}(\nabla\varphi)^2 - \alpha\nabla^2\varphi - \tfrac{1}{2}\mathbb{I}\{\varphi\} = 0, \tag{24}$$

where

$$\mathbb{I}\{\varphi\} = \frac{1}{8\pi^2}\int\int\int\int_{-\infty}^{\infty} |k|\ \mathrm{e}^{\mathrm{i}k_y(y-\eta)+\mathrm{i}k_z(z-\zeta)}\ \varphi(\xi,\ \zeta,\ \tau)\ \mathrm{d}k_y\mathrm{d}k_z\mathrm{d}\eta\mathrm{d}\zeta.$$

On a domain, $0 \leqslant y,\ z \leqslant 1$, with periodic boundary conditions, this equation admits solutions of the form $\varphi = -U\tau + \Phi(y,\ z)$, obtained as the superposition of two uniformly propagating pole solutions $\Phi_1(y,\ \tau)$ and $\Phi_2(z,\ \tau)$ of the form (23), namely

$$\varphi(x,\ z,\ \tau) = -\underbrace{(U_1 + U_2)}_{U}\tau + [\underbrace{\Phi_1(y) + \Phi_2(z)}_{\Phi(y,z)}]. \tag{25}$$

The corresponding flame has a tent-shape conformation with ridges or creases formed along its surface, as shown in figure 7.

In summary, the planar flame propagating into a quiescent mixture is stable in narrow domains $L \times L$ with $L < 4\pi\mathcal{L}/(\sigma - 1)$. When the planar flame is unstable, the perturbed flame evolves into a steadily propagating structure which, for weak thermal expansion, is given by

$$x = -[1 + (\sigma - 1)^2 U]S_L t + (\sigma - 1)L\ \Phi(y,\ z).$$

The flame surface consists of a single-peak structure with a sharp crest pointing towards the burned gas region and propagates at a speed larger than the laminar flame speed by an increment $(\sigma - 1)^2 U$ in units of S_L.

4.2. Nonlinear analysis; $\sigma - 1 = \mathcal{O}(1)$

Motivated by the results for weak thermal expansion, a full nonlinear study for finite values of the thermal expansion parameter σ was carried out within the context of the hydrodynamic theory. The flow field is described by the Navier–Stokes equations (15), albeit with a sufficiently small viscosity, but with the $\mathcal{O}(\delta)$ corrections to the RH relations neglected for numerical simplicity (as justified at the end of section 3.1). The general flame speed relation (16) that includes both, curvature and hydrodynamic strain was retained. The numerical implementation of the free-boundary problem is based on a hybrid NS/front-tracking scheme (Rastigejev and Matalon 2006, Creta and Matalon 2011), which has been tested to reproduce

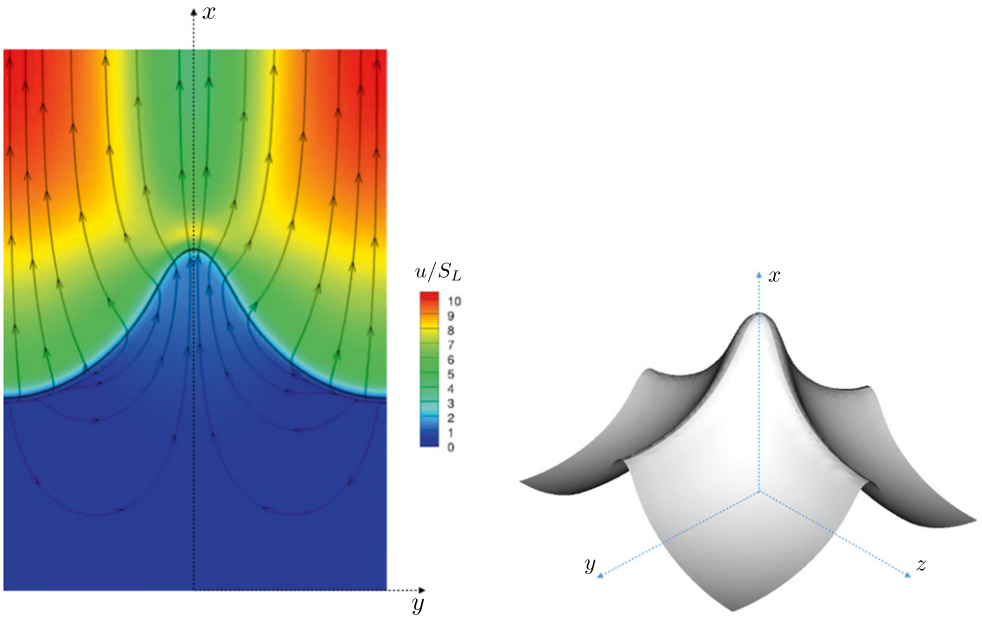

(a) Cusp-like flame in 2D flow field (b) Cusp-like flame in 3D flow field

Figure 8. Steady propagating flames in quiescent mixtures, for $\mathcal{M} < \mathcal{M}_c$. The figure on the left (Reprinted from Fogla *et al* 2017, Copyright (2017), with permission from Elsevier.) also shows the magnitude of the induced flow through the contrast in colors and the flow pattern through selected streamlines.

with sufficient numerical precision the bifurcation characteristics of a planar flame and the small $\sigma - 1$ exact pole solutions of the weakly nonlinear MS equation.

The governing equations were integrated in a sufficiently long (in axial direction) domain of transverse dimension L (in two-dimensions), or of dimension $L \times L$ (in three-dimensions), starting with a slightly perturbed planar flame propagating in a quiescent mixture. Periodic boundary conditions were imposed in all spanwise directions. In dimensionless form, using L, S_L, L/S_L as units of length, speed and time, the problem depends on the Prandtl number (which was kept fixed), the thermal expansion coefficient σ (selected in the range 4–6) and the *Markstein number* $\mathcal{M} \equiv \mathcal{L}/L$. The latter is treated as the bifurcation parameter, since according to linear theory the planar flame is stable for $\mathcal{M} > \mathcal{M}_c$, where

$$\mathcal{M}_c = \frac{1}{2\pi}[(\sigma - 1)\big/(3\sigma - 1)], \tag{26}$$

namely in sufficiently narrow domains, for mixtures with $\mathcal{L} > 0$; see the discussion following the dispersion relation (20).

The long time behavior of the flame front was verified to converge towards a steadily propagating structure of the form

$$x = -(1 + U)S_L t + L\Phi(y, z),$$

where U, as before, is the increment in speed above the speed S_L of the planar flame. For $\mathcal{M} > \mathcal{M}_c$ the planar flame is stable and, indeed, $U \to 0$ and $\Phi(y, z) \to 0$, as $t \to \infty$. For $\mathcal{M} < \mathcal{M}_c$, the flame shape $\Phi(y, z)$ becomes independent of time, as $t \to \infty$, with U tending towards a positive constant value. Figure 8 shows representative flame structures acquired in

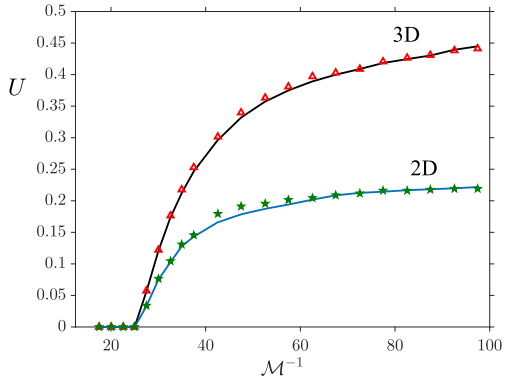

Figure 9. Bifurcation diagram showing the dependence of the increment of the flame propagation speed U (solid lines) and flame surface area (symbols) on the reciprocal of the Markstein number $\mathcal{M}^{-1}$ for flames in two- and three-dimensional flows; calculated for $\sigma = 5$.

two- and three-dimensional flows. The flame front acquires a cusp-like conformation pointing towards the burned gas region and propagates (downwards) towards the fresh mixture at a constant speed. Compared to the pole solutions the crests are more rounded, but become significantly sharper for smaller values of $\mathcal{M}$. Figure 8(a) also illustrates the induced flow resulting from gas expansion of a cusp-like flame. The color shades correspond to the magnitude of the axial velocity component and the solid lines to selective streamlines. The graph shows the deflection of streamlines across the flame, resulting from the large jump in the gas velocity component normal to the flame front, and the vortical flow induced in the unburned gas (otherwise at rest), which is responsible for sustaining the sharp cusp by advecting towards the crest the mixture from the shallow troughs. The propagation speed of the two-dimensional surface in a 3D flow field is nearly twice the speed of the one-dimensional curve representing the flame surface in a 2D flow field.

The effect of systematically reducing $\mathcal{M}$, or increasing the *reciprocal* of the Markstein number $\mathcal{M}_c$, is illustrated in the bifurcation diagram of figure 9, following Patyal and Matalon (2018). The graph corresponds to $\sigma = 5$, for which $\mathcal{M}_c^{-1} \approx 21.98$, and displays the dependence of the increment in propagation speed U, and associated increase in surface area, of the *stable* flames on $\mathcal{M}^{-1}$ in two- and three-dimensional flows. For sub-critical conditions the stable flames are planar and propagate at the laminar flame speed, such that $U = 0$. For super-criticial conditions, the *stable* flames are cusp-like conformations that become taller with sharper crests when increasing $\mathcal{M}^{-1}$. The increase in propagation speed is directly related to the larger surface area that the flame develops when $\mathcal{M}^{-1}$ increases.

5. Turbulent flames

It has been suggested for some time, based on experimental studies, that the hydrodynamic, or DL instability has an effect on the propagation speed of turbulent flames (Paul and Bray 1996, Kobayashi *et al* 1998, Al-Shahrany *et al* 2006). This effect, however, has been invariably neglected in theoretical studies; and, although it is implicitly included in numerical simulations, its role in such studies has not been clearly singled out. Since the Markstein number, which has clearly delineated the role of the instability under laminar conditions, is a parameter in the hydrodynamic theory, the model is well-suited to depict the influence of the DL

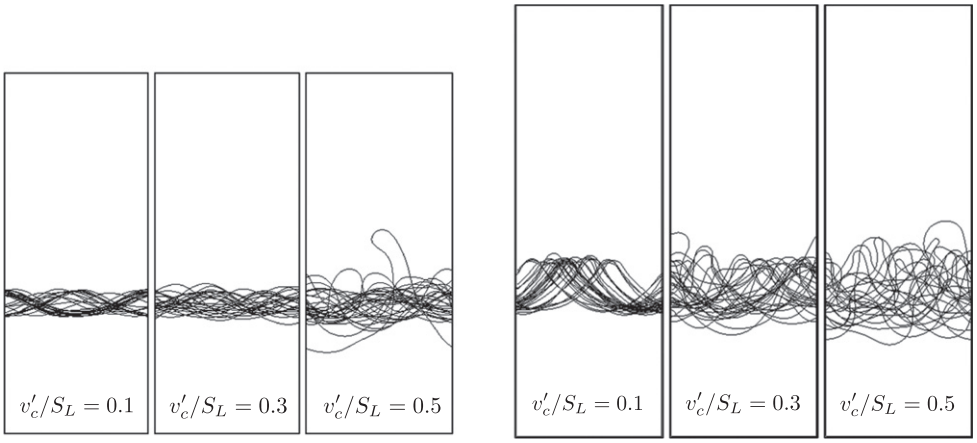

(a) Sub-critical ($\mathcal{M} > \mathcal{M}_c$) flames (b) Super-critical ($\mathcal{M} < \mathcal{M}_c$) flames

Figure 10. Turbulent flames for sub-critical and super-critical conditions; the figure shows the extent of the flame brush for various turbulence intensities v_c'/S_L. Reprinted from Fogla *et al* (2015), Copyright (2015), with permission from Elsevier.

instability on turbulent flames. The objective is therefore to examine the propagation of a premixed flame into a homogeneous, isotropic, turbulent flow of zero mean—the equivalent of a quiescent mixture in the laminar setting, in a sufficiently long domain of transverse dimension L. The pre-generated turbulent flow is characterized by a turbulence intensity v_c'/S_L, measured by the root mean square of the velocity fluctuations in units of the laminar flame speed, and an integral scale that represents the average eddy size which has been kept fixed; details can be found in Creta and Matalon (2011). Periodic boundary conditions are imposed in the spanwise direction, so that the flame segment considered may be viewed as a basic building block of a larger freely-propagating turbulent flame, devoid of the effects of a particular experimental configuration. The mean propagation speed of the fluctuating flame is then appropriately defined as the *turbulent flame speed*.

Although the notion of stability/instability for turbulent conditions cannot be rigorously defined as for laminar flows, the conformation of the flame brush and the turbulent propagation speed are found to change drastically when $\mathcal{M}^{-1}$ increases above a critical value, approximately equal to the bifurcation parameter $\mathcal{M}_c^{-1}$ determined from linear stability theory. In figure 10 we show the turbulent flame brush for increasing values of the turbulence intensity for two distinct values of the Markstein number. The flame brush consists of a superposition of instantaneous flame fronts over a specified time interval. At subcritical conditions, the flame brush remains on the average planar; i.e., it is equally concave as it is convex, or the probability density function of the curvature is symmetrically distributed around a zero mean. The turbulent flame speed increases with turbulent intensity due to the larger surface area of the fluctuating flame but tends to one, when $v_c'/S_L \to 0$. It is evident that under such conditions the turbulent propagation is not affected by the DL instability. At supercritical conditions, the flames attain a distinct cusp-like conformation, reminiscent of the cusp-like structures observed under laminar conditions, Due to the low turbulence intensities the flow seems to only translate the flame, since it is not sufficiently energetic to significantly deform it. The flame brush has therefore an overall robust appearance, hardly affected by the turbulence. The turbulent flame speed is noticeably larger due to the larger flame surface area

induced by the DL instability, and increases with increasing turbulence intensity. However, in this case it tends to a constant larger than one when $v_c'/S_L \to 0$, corresponding to the propagation speed of the cusp-like flame shown in figure 9.

When increasing the turbulence intensity to higher levels, the influence of the DL instability on the super-critical mode of propagation progressively decreases to a point that it has no longer a visible effect on the turbulent flames. The increment in turbulent flame speed between the two cases diminishes when the turbulence level increases indicating that the DL mechanism is progressively weakened and overshadowed by the turbulence. These observations have been further substantiated by detailed examination of various statistical flame characteristics. Recent experimental studies (Al-Shahrany *et al* 2006, Bradley *et al* 2013) have also pointed out the limited range of dominance of the DL instability in a turbulent setting.

6. Conclusions

Treating a flame as a surface of density discontinuity, Darrieus and Landau concluded in their seminal work that due to gas expansion planar flames are unconditionally unstable. Effects due to the finite thickness of the flame, introduced phenomenologically by Markstein and more systematically using asymptotic methods, led to an understanding of the effects of the diffusion processes occurring inside the flame zone on its stability. Specifically, it was established that diffusion influences act to stabilize the short wavelength disturbances in mixtures that are deficient in the less mobile reactant, or mixtures with positive Markstein length. Long wavelength disturbances are amplified by the DL instability, unless they are suppressed due to the finite transverse size of the domain within which the flame is propagating.

The implication from the Darrieus and Landau publications is that the instability of a flame front leads in itself to turbulence. Darrieus has further stated in a letter accompanying the submission of his paper to the Sixth International Congress of Applied Mechanics that, although the prediction of turbulence is essential and confirms the expectation of an ideal fluid, it is paradoxical that the introduction of viscosity in the calculation does not assure stability. The evidence from a weakly nonlinear theory, and from numerical simulations of a fully-nonlinear model is that the instability does not lead directly to turbulent flames; instead cusp-like conformations with elongated intrusions pointing towards the burned gas are formed. These structures, which become taller with sharper peaks when the Markstein number (the ratio of the Markstein length to the domain size) decreases, propagate much faster than the laminar flame speed and may reach speeds 20%–50% faster than the speed of a planar flame. The DL instability has also an influence on the topology and propagation speed of turbulent flames. For super-critical conditions, the flame brush is much thicker than its nearly-planar appearance in the absence of the instability, consists of fluctuating highly-corrugated cusp-like structures that are the hallmark of the instability, and propagates at a speed that is enhanced by the turbulence and further augmented by the instability. The DL influence on turbulent flames, however, appears limited to low-to-moderate turbulence intensities. Finally, we note that the nonlinear development of premixed flames under the combined effects of hydrodynamic and thermo-diffusive instabilities has not been extensively studied and remains poorly understood.

Appendix

We present below the coefficients appearing in the dispersion relation (19) for two special cases. For constant transport properties, or $\tilde{\lambda}(x) \equiv 1$, we have

$$B_1 = \frac{\sigma}{2}\left\{\frac{(\sigma + 1 + 2\omega_{\rm DL})\frac{\sigma \ln \sigma}{\sigma - 1} + \sigma - 1}{\sigma + (\sigma + 1)\omega_{\rm DL}}\right\},$$

$$B_2 = \frac{\sigma}{2}\frac{(1 + \omega_{\rm DL})(\sigma + \omega_{\rm DL})}{(\sigma - 1)[\sigma + (\sigma + 1)\omega_{\rm DL}]}\int_1^\sigma \frac{\ln x}{x - 1}{\rm d}x,$$

$$B_3 = 0$$

which are identical to the results presented in Matalon and Matkowsky (1982). For comparison note that q, ϵ and le in the referenced paper are equivalent to $\sigma - 1$, $(\sigma - 1)/\beta$ and $\beta({\rm Le} - 1)/(\sigma - 1)$, respectively.

For variable transport, with $\tilde{\lambda}(T) \sim T$, we have

$$B_1 = \frac{1}{4}\left\{\frac{2\sigma^2(\sigma + 1 + 2\omega_{\rm DL}) + \sigma^3 - \sigma}{\sigma + (\sigma + 1)\omega_{\rm DL}}\right\},$$

$$B_2 = \frac{\sigma}{2}\left\{\frac{(1 + \omega_{\rm DL})(\sigma + \omega_{\rm DL})}{\sigma + (\sigma + 1)\omega_{\rm DL}}\right\},$$

$$B_3 = \frac{\sigma}{2}\left\{\frac{(\sigma - 1)^2}{\sigma + (\sigma + 1)\omega_{\rm DL}}\right\}.$$

which appeared in Matalon *et al* (2003) with a minor typo in B_2 (the extra factor $\sigma - 1$ in the numerator must be removed).

References

Al-Shahrany A, Bradley D, Lawes M, Liu K and Woolley R 2006 Darrieus–Landau and thermo-acoustic instabilities in closed vessel explosions *Combust. Sci. Technol.* **178** 1771–802

Altantzis C, Frouzakis C, Tomboulides A, Matalon M and Boulouchos K 2012 Hydrodynamic and thermodiffusive instability effects on the evolution of laminar planar lean premixed hydrogen flames *J. Fluid Mech.* **700** 329–61

Barenblatt G, Zel'dovich Y and Istratov A 1962 On the diffusional thermal instability of laminar flames *Prikl. Mekh. Tekh. Fiz.* **2** 21

Bradley D, Lawes M, Liu K and Mansour M S 2013 Measurements and correlations of turbulent burning velocities over wide ranges of fuels and elevated pressures *Proc. Combust. Inst.* **34** 1519–26

Bush W and Fendell F 1970 Asymptotic analysis of laminar flame propagation for general Lewis numbers *Combust. Sci. Technol.* **6** 421–8

Creta F and Matalon M 2011 Strain rate effects on the nonlinear development of hydrodynamically unstable flames *Proc. Combust. Inst.* **33** 1087–94

Creta F and Matalon M 2011 Propagation of wrinkled turbulent flames in the context of hydrodynamic theory *J. Fluid Mech.* **680** 225–64

Darrieus G 1938 Propagation d'un front de flamme La Technique Moderne (Paris) and in 1945 at Congrès de Mécanique Appliquée, Unpublished work

Eckhaus W 1961 Theory of flame front stability *J. Fluid Mech.* **10** 80–100

Fogla N, Creta F and Matalon M 2015 Effect of folds and pockets on the topology and propagation of premixed turbulent flames *Combust. Flame* **162** 2758–77

Fogla N, Creta F and Matalon M 2017 The turbulent flame speed for low-to-moderate turbulence intensities: hydrodynamic theory versus experiments *Combust. Flame* **175** 155–69
Frankel M and Sivashinsky G 1982 The effect of viscosity on hydrodynamic stability of a plane flame front *Combust. Sci. Technol.* **29** 207–24
Frouzakis C, Fogla N, Tomboulides A, Altantzis C and Matalon M 2015 Numerical study of unstable hydrogen/air flames: shape and propagation speed *Proc. Combust. Inst.* **35** 1087–95
Gutman S and Sivashinsky G 1990 The cellular nature of hydrodynamic flame instability *Physica* D **43** 129–39
Kobayashi H, Kawabata Y and Maruta K 1998 Experimental study on general correlation of turbulent burning velocity at high pressure *Proc. Combust. Inst.* **27** 941–8
Landau L D 1944 On the theory of slow combustion *Acta Physicochim. USSR* **19** 77
Mallard E and Chatelier H L 1883 Recherches expérimental et théorique sur la combustion des mélanges gazeux explosifs *Ann. des Mines, 8é* **IV** 274–561
Markstein G H 1951 Experimental and theoretical studies of flame front stability *J. Aeronaut. Sci.* **18** 199–209
Markstein G H 1964 *Nonsteady Flame Propagation : AGARDograph* vol 75 (Amsterdam: Elsevier)
Matalon M 1983 On flame stretch *Combust. Sci. Technol.* **31** 169–81
Matalon M, Cui C and Bechtold J K 2003 Hydrodynamic theory of premixed flames: effects of stoichiometry, variable transport coefficients and arbitrary reaction orders *J. Fluid Mech.* **487** 179–210
Matalon M and Matkowsky B 1982 Flames as gasdynamic discontinuities *J. Fluid Mech.* **124** 239–59
Matalon M and Matkowsky B J 1983 Flames in fluids: their interaction and stability *Combust. Sci. Technol.* **34** 295–316
Michelson D and Sivashinsky G 1977 Nonlinear analysis of hydrodynamic instability in laminar flames: II. Numerical experiments *Acta Astronaut.* **4** 1207–21
Patyal A and Matalon M 2018 Nonlinear development of hydrodynamically-unstable flames in three-dimensional laminar flows *Combustion and Flame* (in press)
Paul R and Bray K 1996 Study of premixed turbulent combustion including Landau–Darrieus instability effects *Proc. Combust. Inst.* **26** 259–66
Pelce P and Clavin P 1982 Influence of hydrodynamics and diffusion upon the stability limits of laminar premixed flames *J. Fluid Mech.* **124** 219–37
Rahibe M, Aubry N and Sivashinsky G I 1996 Stability of pole solutions for planar propagating flames *Phys. Rev.* E **54** 4958–72
Rastigejev Y and Matalon M 2006 Nonlinear evolution of hydrodynamically unstable premixed flames *J. Fluid Mech.* **554** 371–92
Rastigejev Y and Matalon M 2006 Numerical simulation of flames as gas-dynamic discontinuities *Combust. Theory Modelling* **10** 459–81
Sivashinsky G I 1977a Diffusional-thermal theory of cellular flames *Combust. Sci. Technol.* **15** 137–45
Sivashinsky G I 1977b Nonlinear analysis of hydrodynamic instability in laminar flames: I. Derivation of basic equations *Acta Astronaut.* **4** 1177–206
Thual O, Frisch U and Hénon M 1985 Application of pole decomposition to an equation governing the dynamics of wrinkled fronts *J. Physique* **46** 1485–94
Vaynblat D and Matalon M 2000a Stability of pole solutions for planar propagating flames: I. Exact eigenvalues and eigenfunctions *SIAM J. Appl. Math.* **60** 703–28
Vaynblat D and Matalon M 2000b Stability of pole solutions for planar propagating flames: II. Properties of eigenvalues/eigenfunctions and implications to stability *SIAM J. Appl. Math.* **60** 703–28
Williams F 1985 *Combustion Theory* 2nd edn (Menlo Park, CA: The Benjamin/Cummings)
Zel'dovich Y and Frank-Kamenetsky D 1938 A theory of thermal flame propagation *Zh. Fiz. Khim.* **12** 100–5